Influence of process variables on foaming ability of surfactants: Experimental study and dimensional analysis

Rémy Bois, Océane Adriao, Guillaume Delaplace, Isabelle Pezron, Alla Nesterenko, Elisabeth Van-Hecke

Influence of process variables on foaming ability of surfactants: experimental study and dimensional analysis

Rémy Bois[1]*, Océane Adriao[1], Guillaume Delaplace[2], Isabelle Pezron[1], Alla Nesterenko[1], Elisabeth van-Hecke[1]

[1]*Sorbonne Universités, Université de Technologie de Compiègne, ESCOM, EA 4297 TIMR, rue du Dr Schweitzer, 60200 Compiègne, France*

[2]*Unité Matériaux et Transformations (UMET) – UMR 8207, INRA, Team PIHM, 369 rue Jules Guesde, 59650 Villeneuve d'Ascq, France*

* Corresponding author: alla.nesterenko@utc.fr

Abstract

By applying the dimensional analysis approach to a lab-scale stirred tank process, the influence of process parameters on the foamability of three model surfactants: SLES, Tween 20 and Brij L23 is investigated and modelled. For validation of process law, the theoretical approach is complemented with an experimental work varying process parameters such as agitator rotational speed rate (N), mixing time (t_m) and bottom clearance (C_b). The foam rate of expansion of surfactant solutions is correlated with success to two dimensionless numbers: the Reynolds number and the mixing time number. Reynolds number is observed as mainly governing the amount of formed foam. A clear difference between the intermediate flow regime ($Re < 10^5$) and the turbulent one ($Re > 10^5$) is observed leading to a different process law for each regime. Master curves are finally drawn and can be used for helping to predict final foam volumes in the studied experimental domain according to both dimensionless numbers.

Keywords: foaming, dimensional analysis, Reynolds number, surfactant, process, mechanical stirring

1. Introduction

Numerous technics exist to disperse a gaseous phase into a liquid phase and to generate a foam (Pugh 2016): air incorporation by mechanical stirring (surface aeration), growing bubbles by gas injection, nucleation or chemical reactions. Among them, bubble formation and break-up under shear has been widely studied. In case of surface aeration with mechanical rotating devices, introduction of gas is driven by process parameters such as the rotational speed of the agitator, and is facilitated by the reduced pressure in regions close to rotating blades, induced by the liquid motion. The foaming solution and the gas are strongly sheared to create foam of generally submillimetric bubbles (Drenckhan et al. 2015). Mechanisms of small bubbles formation have been well described in the literature (Müller et al. 2008, Drenckhan et al. 2015). During the first steps of agitation, air at the liquid surface is brought into the solution and enables formation of large bubbles. Under shear, bubbles are then deformed into an elongated shape whose size depends on fluid properties, on the ability of surface agent (surfactants, proteins, polymers) to stabilize the interface, and on imposed shear flow (Stone 2003, Cristini et al. 2004). At a critical size, the bubble breaks and forms smaller bubbles (Müller et al. 2008).

The challenging issue concerning these mechanical devices is generally to obtain foams with desired bubble size and gas fraction, all along with energy efficiency (low power consumption). Three main types of mechanical agitators are often studied when foam generation is considered. The first of them is the planetary mixer, or commonly called kitchen blender, broadly used in the whipping of food foams (Camacho et al. 1998, Massey et al. 2001, Jakubczyk et al. 2006, Müller et al. 2007, Delaplace et al. 2012, Chesterton et al. 2013). Such device allows obtaining very small bubbles (diameters between 0.01 mm and 1 mm), leading to the white aspect of the final foam. Continuous rotor-stator mixers are also found to be efficient for foam generation (Kroezen et al. 1988, Hanselmann et al. 1998, Müller-Fischer

et al. 2005). In such devices, the foaming process is carried out in a relatively small mixing space between a rotor and a stator, both with pins, and gas injection is continuous and controlled. The optimal design of the set is largely discussed, depending on the fluids involved. Finally, stirred tanks with various impellers and coupled or not to gas sparging are also used to produce a foam (Hu et al. 2003, Indrawati et al. 2008, Wu et al. 2012, Celani et al. 2018). In such devices, the impeller type (blade, turbine or propeller) and size greatly influence the fluid flow pattern and so the foaming properties of the solution.

The influence of mechanical agitation process parameters in stirred vessels and the understanding of mechanisms for foam formation have been discussed for years. The literature has shown that the bubble size is a particular foam property and as a consequence is often employed as a target variable for studying the effect of different process parameters. It was shown for various kinds of foams that average bubble diameter generally decreases with an increase of agitation speed due to higher shear and turbulence (Machon et al. 1997, Hu et al. 2003, Indrawati et al. 2008, Wu et al. 2012, Celani et al. 2018). However, Samaras et al. (Samaras et al. 2014) found that in the presence of surfactant solutions, bubble size was not affected by agitation speed. Furthermore, the bubble size can reach a constant value at high agitation speed as well as at long enough residence time which has been explained by a dynamic equilibrium between breakage and coalescence (Hu et al. 2003, Wu et al. 2012). On the contrary, other study demonstrated no influence of coalescence/breakage phenomena from their observed data (Samaras et al. 2014). In addition, some of the authors highlighted that foam bubble size was mainly affected by the volumetric energy input. The energy involved is related to different variables, such as for example rotor speed, mixing time, fluid viscosity and density (Delaplace et al. 2015).

Otherwise, analysis of scientific papers dealing with foaming reveals that properties other than bubble size are used to characterize foaming properties of a surfactant solution. Among

others, one can distinguish foaming capacity, sometimes expressed as gas hold-up or overrun. All those terms are indicators of final amount (volume or height) of foam generated. The amount of produced foam is related to process variables for mechanical agitation method in several studies (Delaplace et al. 2012, Samaras et al. 2014, Celani et al. 2018). An increase of foam volume is observed when increasing rotational speed (Samaras et al. 2014, Celani et al. 2018). Indrawati et al. (Indrawati et al. 2008) used foam density as indicator of foamability and found a decrease of density with increasing speed rate which is in agreement with other studies (Samaras et al. 2014, Celani et al. 2018).

Besides process parameters, the foaming behavior of amphiphilic molecule is governed by its chemical structure, adsorption properties and solution characteristics. In foaming processes, the increase in viscosity of aqueous solution usually leads to the slowdown of foam destabilization, helping reduce bubble size (Ding et al. 2019, Santini et al. 2019), prevent liquid drainage and bubble coalescence (Mohanan et al. 2020, Zhu et al. 2021). Regarding the amount of produced foam, there is no general tendency relating this parameter with viscosity of solution or with equilibrium surface tension of surfactant at CMC (γ_{CMC}). In the case of protein stabilized foams, viscosity and foam amount are generally increased for higher pH values (Mohanan et al. 2020). Kanokkarn et al (Kanokkarn et al. 2017) demonstrated that this trend is strongly affected by the surfactant structure variation: for a series of methyl ester sulfonate with different alkyl chain length, foamability increases for higher γ_{CMC} values, whereas for a series of polyoxyethylated dodecyl alcohol with variable head group size, foamability decreases when γ_{CMC} raises.

Besides these studies on foaming processes, an important use of modelling by dimensional analysis have emerged to further investigate the mixing processes (Zlokarnik 1998, Delaplace et al. 2015) since the pioneer work of Nagata et al. (Nagata et al. 1957). This approach brought better apprehension of mixing mechanisms taking place in a batch reactor, is still

applied nowadays and allowed scaling rules for design of mixing operations (Hsu et al. 1996, Manjula et al. 2010, André et al. 2012, Pradilla et al. 2015). Modelling mixing operations through dimensional analysis has the advantage not to be constrained to a specific type of agitated media (i.e monophasic liquid, liquid/liquid dispersion, gas/liquid dispersion, powders) or to be applied only for classical batch mixing systems (i.e with an agitator rotating around a vertical axis centrally located in the tank). For example, Delaplace et al. (Delaplace et al. 2018) applied the approach for the homogenization of Newtonian miscible liquids in soft elastic reactor that induces mixing by vibration of the tank wall while André et al. (André et al. 2012) performed it for the homogenization of powders agitated with a planetary mixer. The effect of emulsification process parameters and development of quantitative correlation with microspheres size were also investigated by this as well as the scale-up prediction (Hsu et al. 1996). Otherwise, this method of modelling was applied for studying foam elaboration in a continuous mixing equipment (Mary et al. 2013) and spray drying of maltodextrin solutions (Lachin et al. 2020).

From the only analysis of the exhaustive works of Delaplace & al. dealing with modelling mixing operations by dimensional analysis, it appears that a lot of dimensional target variables can be chosen to describe the evolution of the mixing system and relate them to the causal dimensional physical quantities responsible for the evolution of the mixing system through process relationship: heat transfer coefficient (Delaplace et al. 2001), power consumption (Delaplace et al. 2005, Delaplace et al. 2007), mixing time (Delaplace et al. 2007), volumetric gas–liquid mass transfer coefficient (Hassan et al. 2012), gas hold up (Delaplace et al. 2012). Moreover, using dimensionless numbers can be interesting for scaling-up processes. Indeed, clear guidelines exist to evaluate whether a condition of similarity occurs between the model and the prototype. These conditions of similarity require the equality of the numerical value of each dimensionless number involved on both scales as

remembered in lots of books on the subject (Zlokarnik 1998, White 2001, Szirtes et al. 2007, Delaplace et al. 2015). In this sense, dimensional analysis allows us to dispose of a scientific frame for scaling-up.

Beyond the fact that dimensional analysis can provide scaling laws, modelling by dimensional analysis is ever interesting at lab-scale for discriminating different surfactants abilities as reducing the number of experiments for obtaining process relationship. Moreover, in depth understanding the relation between the parameters responsible for foam formation process and the amount of produced foam has direct relevance for the choice of surfactant. At this stage, to be in ability to select surfactants for foaming formulation requires additional and accurate knowledge about the specific role played by all physical quantities (arising from process, geometry of mixing equipment and agitated media) involved in the foaming operation.

Up to date, only a few scientific studies have focused on dimensional analysis of foaming process in agitated vessels. Machon et al. (Machon et al. 1997) summarized the basis for dimensional correlations between bubble size and process-product parameters considering bubble break-up processes on the one hand and coalescence processes on the other hand. Those correlations mainly involve rotation speed, impeller diameter, power input, liquid volume, density, viscosity and surface tension and foam volume. Smith (Smith 1992) gathered data from various authors and showed that in many cases, gas holdup is correlated with sufficient accuracy in a monomial form to Reynolds number (Re), Froude number (Fr), gas flow number (Flg), and a geometrical dimensionless number characterizing the position of the impeller in the tank. However this single monomial relationship does not take into account mixing time nor surfactants solution properties like surface tension. The same remark can be done from the work of Delaplace et al. (Delaplace et al. 2012) with planetary mixer since only one recipe was carried out as the foaming solution, even if in this case the mixing time effect was discussed.

In the present study, a dimensional analysis of a lab-scale stirred tank process is carried out in view of establishing a causal relationship between foaming properties of surfactants solutions, especially their foaming ability, and process variables. This theoretical approach is complemented with an experimental work varying process parameters and measuring the evolution of foam height with mixing time in order to validate the obtained semi-empirical correlations. Three model surfactants solutions at their critical micellar concentration (CMC) were foamed. Such a study aims at a better understanding of which of the physical phenomena mainly control foam formation in a classic mechanical agitator.

Nomenclature

Ca	Capillary number	R_e	Reynolds number
C_b	bottom clearance of the agitator (m)	T	tank diameter (m)
d	agitator diameter (m)	t_m	mixing time (s)
Fr	Froude number	W_e	Weber number
g	constant of gravity ($m.s^{-2}$)	γ	surface tension
H_F	height of foam generated (m)	η	liquid Newtonian viscosity (Pa.s)
H_L	liquid height in the tank (m)	ρ	liquid density ($kg.m^{-3}$)
N	rotational speed of agitator (s^{-1})	Θ_m	mixing time number

2. Experimental setup

2.1. Surfactants solutions

Tween 20 (> 97 %, M_w=1227.5 $g.mol^{-1}$), Brij L23 (> 98 %, M_w=1198 $g.mol^{-1}$) were purchased from Sigma-Aldrich and used without further purification. SLES (M_w=370 $g.mol^{-1}$) was provided from THOR Personal Care SAS (La Croix Saint-Ouen, France) as 27 wt % aqueous solution (Texapon® NSO UP). Ultrapure water with a resistivity of 18.2 MΩ.cm

produced by a PureLab Classic purification chain (Elga/Veolia, Wissous, France) was used for all analysis. Model solutions at different concentrations were prepared by dissolving a known quantity of pure surfactant in ultrapure water.

2.2. Critical micellar concentration determination

The measurement of surface tension at equilibrium (γ_{eq}) were obtained using K100 Krüss tensiometer (Hamburg, Germany) equipped with a Wilhelmy platinum plate (length 10 mm, width 19.9 mm, thickness 0.2 mm). The tensiometer operates by holding a plate in a fixed vertical position attached to a microbalance. The microbalance measures the force acting on the plate, which is used for the calculation of surface tension. The resolution of the microbalance for all measurements is of 10 µg, which corresponds to a resolution of 0.0024 $mN.m^{-1}$ on the surface tension scale. The sample solution was put in a glass vessel surrounded by a circular thermostated system maintained at 25 ± 1°C. Prior to each determination, the plate was rinsed with ethanol and water, and burnt to red-hot conditions in a blue flame to ensure perfect wetting (zero contact angle). The measurement of surface tension at the air/liquid interface was carried out by submerging a Wilhelmy plate in the solution during several minutes (time required to reach an equilibrium surface tension (γ_{eq}). All measurements were repeated at least three times. The Critical Micellar Concentration (CMC) of each surfactant was determined from the break point of concentration-surface tension curve. CMC values obtained are listed below and were similar to values from literature:

- SLES: 0.5 mM (Rosen et al. 1996)
- Tween 20: 0.04 mM (Patist et al. 2000)
- Brij L23: 0.07 mM (Patist et al. 2000, Wang et al. 2005)

192 *2.3. Foaming method*

193 The foaming experiments were performed with surfactants solutions at critical micellar
194 concentration (CMC). As CMC of all studied solutions was lower than 1mM, density (ρ) and
195 viscosity (η) could be assumed constants and equal to those of water: 10^3 $kg.m^{-3}$ and 0.001
196 $kg.m^{-1}.s^{-1}$ respectively. A mechanical stirrer (IKA Eurostar20 high speed digital, IKA
197 Labortechnik, Staufen, Germany) equipped with a 4-bladed stirring element R1342 (diameter:
198 5 cm) was used for the present study. 100 mL of a fresh solution were placed in a 600 mL
199 beaker (diameter of beaker: 9 cm; initial liquid height, H_L: 2.8 cm). Stirrer was fixed at
200 different heights (1 – 2.8 cm) from beaker bottom. Agitation was applied at various speeds
201 (70 – 6000 rpm) for different mixing times (30 – 300 s). Foaming ability of surfactant was
202 characterized by measuring foam height (H_F) directly after the end of agitation process.
203 Measurement of foam heights was realized visually from the graduated beaker. Foam rate of
204 expansion expressed as the ratio of generated foam height over initial liquid height (H_F/H_L)
205 was chosen as target dimensionless variable. Experiments were carried out in triplicates.
206

207 **3. Dimensional analysis**

208 The dimensional analysis of mechanical stirring process applied to foam formation was
209 performed according to the methodology described by Delaplace et al. (Delaplace et al. 2015).
210

211 *3.1. Physical variables involved in the process*

212 Experimental variables that might influence the foam height (H_F) were identified, as a first
213 step of dimensional analysis. One can distinguish four kinds of physical quantities involved in
214 the process as illustrated in Fig. 1.

215 - Parameters related to surfactant solution: density (ρ), viscosity (η) and equilibrium
216 surface tension (γ_{eq});

- Process parameters: mixing time (t_m) and agitator rotational speed rate (N);
- Geometrical parameters, giving information related to the domain of flow application: tank diameter (T), stirrer diameter (d), initial liquid height (H_L) and bottom clearance (C_b);
- Boundary conditions applied to the studied mixing system: here, gravitational acceleration (g) is the only boundary condition and, as explained in numerous articles dealing with modelling by dimensional analysis, it should not be omitted even if this physical dimensional quantity is in fact a dimensional constant in the study (Zlokarnik 1998, White 2001, Szirtes et al. 2007, Delaplace et al. 2015).

Thus, the foam height can be described as a function of all those physical quantities in a so-called process law, as expressed in Eq. 1.

$$H_F = f_1(\rho, \gamma_{eq}, \eta, N, t_m, T, d, H_L, C_b, g) \quad \text{Eq. 1}$$

3.2. Dimensionless numbers involved in the process

All variables can be expressed according to three basic dimensions: time, length and mass. A physical quantity (H_F) that is a function of ten others described by three fundamental dimensions (mass, time, length) can be described by a new function of 7 dimensionless numbers (Delaplace et al. 2015). A dimensional analysis enables to obtain such numbers as indicated in the Buckingham π theorem (Zlokarnik 1998, White 2001, Szirtes et al. 2007, Delaplace et al. 2015). Such set of dimensionless numbers, also called π-numbers, can be obtained by:

Step 1: Listing dimensions of all variables.

Step 2: Choosing a set of repeated variables, called the base. The repeated variables should be dimensionally independent and covering all the dimensions of the

dimensional variables encountered in the studied system. The choice of the base is multiple and up to the user.

Step 3: Dividing each non-repeated variable by a product of repeated variables raised to various exponent to obtain each dimensionless number. Algebraically, it consists to find the exponents which make the product dimensionless.

Step 4: Rearranging the dimensionless numbers by raising it to any power and multiplying it by other dimensionless numbers raised to different power. Recombinations are possible and let the user find different set of π-numbers for a given studied system The most common reasons associated to recombinations are i) to give rise to common dimensionless numbers ii) to eliminate a physical quantity of a dimensionless number in order to obtain a new dimensionless number independent of this physical quantity .

The reader must retain that the choice of the base and rearrangements are multiple and up to the user. Nevertheless, these choices will not affect the content of the data but only the form of their presentation. These common 4 steps of modelling by dimensional analysis for constructing a set of dimensionless numbers are mathematically explained and justified in numerous books in which the reader can refer whether he would like to go further (Zlokarnik 1998, White 2001, Szirtes et al. 2007, Delaplace et al. 2015) so we will not detail them here in depth.

In the following section, we will use this rule allowed by dimensional analysis to illustrate and discuss particulate effects of the results. For our case, choosing the base (ρ, N, H_L) leads to a set of seven dimensionless numbers for explaining the chosen dimensionless target variable, H_F/H_L, also known as the foam rate of expansion, as follows:

$$\frac{H_F}{H_L} = f_2\left(\pi_1 = \frac{\eta}{\rho.N.H_L^2}, \pi_2 = \frac{\gamma_{eq}}{\rho.N^2.H_L^3}, \pi_3 = \frac{g}{N^2.H_L}, N.t_m, \pi_4 = \frac{d}{H_L}, \frac{T}{H_L}, \frac{C_b}{H_L}\right) \quad \text{Eq. 2}$$

Rearranging leads to a set of seven dimensionless numbers, including Reynolds, Froude and Capillary numbers and mixing time number:

$$\frac{H_F}{H_L} = f_3(\mathrm{Re} = {\pi_1}^{-1}.{\pi_4}^2, \mathrm{Ca} = {\pi_1}^{-1}.\pi_4.\pi_2, \mathrm{Fr} = {\pi_3}^{-1}.\pi_4.\pi_2, \Theta_m, \frac{d}{H_L}, \frac{T}{H_L}, \frac{C_b}{H_L}) \quad \text{Eq. 3}$$

with, $\mathrm{Re} = \frac{\rho.N.d^2}{\eta}$, the Reynolds number, $\mathrm{Ca} = \frac{\eta.N.d}{\gamma_{eq}}$, the Capillary number, $\mathrm{Fr} = \frac{N^2.d}{g}$, the Froude Number, and $\Theta_m = N.t_m$, the mixing time number.

Each dimensionless number appearing in Eq. 3 is a measure of the non-repeated variables, respectively (liquid height, viscosity, equilibrium surface tension, gravitational acceleration, agitator diameter, tank diameter, bottom clearance) and has consequently a precise physical meaning. For instance, Reynolds number represents the ratio of inertial stress over viscous stress; Capillary number is defined by the ratio of viscous stress over interfacial stress and account for the effect of surface tension. Finally, the Froude number is the ratio of the inertial force divided by gravitational force. This number is supposed to describe how the liquid free surface is deformed and how the vortex rise when the impeller rotational speed increases. Θ_m represents the number of revolutions achieved by the agitator for obtaining the given height of foam and measures the effect of time on dynamic foam process.

Rearrangement of Eq. 3 could be performed in order that impeller rotational speed is involved only in one dimensionless number. For example, replacing Froude number, Fr, by $\mathrm{Fr}^{-1}\mathrm{Re}^2$, allows appearing another well-known dimensionless number: the Galilei number, Ga. The Galilei number ($= \frac{d^3.g.\rho^2}{\eta}$) also measures gravitational effect but this time independently of impeller rotational speed. In the same way, it is possible to replace the capillary number Ca by $\mathrm{Ca}^* = \mathrm{Ca}\,\mathrm{Re}^{-1}$ in order that the new dimensionless number, Ca^*, measuring γ_{eq} effect, becomes independent of the agitator rotational speed ($\mathrm{Ca}^* = \frac{\eta^2}{\rho.d.\gamma_{eq}}$).

Consequently, the following π-spaces can be used indifferently to represent and to discuss the results about foaming process in batch reactor:

289 $$\frac{H_F}{H_L} = f_4(Re, Ca, Fr, \Theta_m, \frac{d}{H_L}, \frac{T}{H_L}, \frac{C_b}{H_L})$$ Eq. 4 (idem Eq.3)

290 $$\frac{H_F}{H_L} = f_5(Re, Ca, Ga, \Theta_m, \frac{d}{H_L}, \frac{T}{H_L}, \frac{C_b}{H_L})$$ Eq. 5

291 $$\frac{H_F}{H_L} = f_6(Re, Ca^*, Ga, \Theta_m, \frac{d}{H_L}, \frac{T}{H_L}, \frac{C_b}{H_L})$$ Eq. 6

292

293 As mentioned above, much more π-spaces exist and could be built but only the 3 above ones
294 will be used latter in our discussion.

295

296 *3.3. Establishment of the process relationship relevant to the study*

297 For the present study, as some dimensional variables are held constant during the
298 experimental runs, several levels of simplification were possible in Eq.4 to Eq.6. Tank
299 diameter (T) and stirrer diameter (d) were kept constant, as well as the initial height of
300 surfactant solution (H_L). Therefore, T/H_L and d/H_L remained at constant values. Furthermore,
301 as surfactant solutions were studied at a concentration equal to their CMC (CMC < 1 mM for
302 the three surfactants), density and viscosity were assumed constants and equal to those of pure
303 water. Thereby, Galilei number becomes constant. Consequently, with regards to the specific
304 experimental program applied here, the influence of some dimensionless numbers appearing
305 in Eq.4 to Eq.6 cannot be studied and the reduced π-spaces are now given in Eq. 7 and Eq.8.

306 $$\frac{H_F}{H_L} = f_7(Re, Ca, \Theta_m, \frac{C_b}{H_L})$$ Eq. 7

307 $$\frac{H_F}{H_L} = f_8(Re, Ca^*, \Theta_m, \frac{C_b}{H_L})$$ Eq. 8

308 Dimensional analysis and specific experimental program give rise to reduced π-spaces which
309 may explain the evolution of the target variable (here the amount of foam). However,
310 dimensional analysis doesn't indicate the mathematical form of the process relationship
311 correlating the dimensionless numbers relative to the causes, with the target dimensionless

312 number ($=\frac{H_F}{H_L}$). Since a monomial form function (like Eq. 9) can display a wide spectrum of
313 plots, depending on the values of unknowns ($Const$, a, b, c and d appearing in Eq.9), and
314 minimizes the number of unknowns to be identified, this mathematical equation is often
315 considered to adjust to experimental data (White 2001, Szirtes et al. 2007, Delaplace et al.
316 2015). So this simple form of mathematical equation was attempted in our study for
317 correlating foaming ability of surfactants solutions as a function of process variables.
318 Monomial form applied to Eq. 8 gives Eq. 9:

319 $$\frac{H_F}{H_L} = Const.\,Re^{a}\,Ca^{*b}\Theta_m{}^{c}\left(\frac{C_b}{H_L}\right)^{d} \quad (Const, \text{ a, b, c and d being constants}) \qquad \text{Eq. 9}$$

320 Adjustment of this model to experimental data was performed using the least squares method,
321 allowing to obtain the coefficients ($Const$, a, b, c and d). To evaluate model performance,
322 correlation coefficient (R^2) and mean absolute error (MAE, Eq.10) were calculated.

323 $$MAE=\frac{1}{n}\sum_{i=1}^{n}|y-\hat{y}| \qquad \text{Eq. 10}$$

324 with n, the number of experiments, y and $\hat{y}$ the experimental and predicted expansion rate,
325 respectively.

326

327 **4. Results and discussion**

328 *4.1. Influence of process variables on foaming ability :case of SLES solution*

329 Foaming experiments were carried out for SLES solutions at CMC, by varying the agitation
330 speed (5 levels), mixing time (4 levels) and bottom clearance (3 levels), into 38 assays as
331 reported in Table 1. The results are illustrated in Fig. 2 and Fig. 3.

332 Fig. 2 focuses on the influence of bottom clearance through its associated dimensionless
333 number (C_b/H_L). A C_b/H_L value of 1 means that the agitator was placed at liquid-air interface,
334 C_b/H_L values of 0.2 and 0.5 correspond to the agitator immersed into surfactant solution. For a
335 same agitation process, i.e. fixed time and speed of agitation, Fig. 2 shows that similar rates of

expansion were obtained whatever the bottom clearance. Even when the agitator is entirely immersed in the solution, agitation speed was sufficient to generate enough air-liquid interface and create bubbles. This result shows that the corresponding dimensionless number (C_b/H_L) involved in Eq. 9 has finally little influence on final foam amount.

The influence of Reynolds number on foam expansion rate at $C_b/H_L=1$ is shown in Fig. 3a. A significant increase of the foam rate of expansion (x10 approximately) with increasing the Reynolds number from 3.10^4 to 24.10^4 is observed. A maximum of H_F/H_L is observable at Reynolds values between 10.10^4 and 15.10^4, for all investigated mixing time values (Fig. 3a). A value of Re close to 10.10^4 is usually associated with a transition from intermediate flow regime to turbulent regime for stirred tanks of various configurations (Medek et al. 1979, Hall 2018). This transition might explain a maximum in final foam volumes. In the intermediate regime, an increase of rotation speed facilitates incorporation of air within the liquid, producing more foam. At higher agitation speeds corresponding to turbulent regime, the mixed system probably undergoes too strong turbulence that would induce foam collapse. Thus, the phenomenon of bubbles breakup occurs faster than foam generation, leading to a stagnation then a decrease in height of formed foam.

As shown in Fig. 3b, the mixing time number (Θ_m) has also a significant influence on final foam height. Extending the mixing time number usually allows producing higher amount of foam, by increasing the number of exchanges between gas and liquid, which facilitates creation of interfaces. Furthermore, the obtained results also demonstrated the presence of a plateau for foam volumes. At a certain mixing time number, expansion rate remains constant, at a value that depends on the agitation speed. This result can be put in regards with Bikerman work (Bikerman 1973) in case of a sparging method (gas injection through a frit): the foams reach a plateau value called “foaminess” that depends on gas flow rate. At relatively low flow rates, the amount of formed foam increases proportionally to gas superficial velocity. One can

suppose that the same observation is transposable in the intermediate regime ($Re < 10^5$) for the present study. From Fig. 3, both mixing time and agitation speed play major roles for the formation of foam. For example, considering Θ_m close to 3500, result of the experiment could be significantly different: H_F/H_L of 0.58 for trial 10 (700 rpm for 300 s) and H_F/H_L of 2.97 for trial 22 (3360 rpm for 30 s).

4.2. Fitting the process law to experimental data: case of SLES solution

Considering the only surfactant SLES, at CMC, it is possible to further simplify the generic monomial process law (Eq. 9) since Ca* ($= Ca\,Re^{-1} = \frac{\eta^2}{\rho.d.\gamma_{eq}}$) is constant ($\gamma_{eq}$ being constant here). The form of the resulting process law thus becomes as follows:

$$\frac{H_F}{H_L} = Const.\,Re^{a}\Theta_m{}^{c}\left(\frac{C_b}{H_L}\right)^{d} \quad \text{Eq. 11}$$

Since two regimes of flow were clearly identified as having different consequences on foam expansion rate (Fig. 3a), each of them was considered separately. Firstly, the intermediate flow regime ($10^4 < Re < 10^5$) was considered. The first 20 lines from Table 1 were used to identify the four coefficients: $Const$, a, c and d in that domain. According to the Table 1, it should be noticed that the maximal studied Θ_m was 10^4 in that Re range. Calculations lead to the process relationship expressed in Eq. 12. Model data were in good agreement with experimental points, as presented in Fig. 4a ($R^2 = 0.95$).

$$\frac{H_F}{H_L} = 10^{-7}Re^{1.09}\Theta_m{}^{0.57}\left(\frac{C_b}{H_L}\right)^{0.09} \quad \text{Eq. 12}$$

From the Eq. 12, one should note the small power coefficient for C_b/H_L, reflecting the slight influence of this dimensionless number on expansion rate in the specific experimental area of the study. This result confirmed the observations discussed previously. The agitation speed has the major influence as Reynolds number has the highest coefficient value. From Eq. 12 and definitions of Re and Θ_m, the separate effects of agitation speed N and mixing time t_m can

385 be appreciated. Indeed, the latter physical quantity only appears in Θ_m value. On the other
386 hand, rotational speed is implicated in both dimensionless numbers. As a result, the expansion
387 rate could be viewed as approximately proportional to $N^{3/2}{t_m}^{1/2}$, in the studied intermediate
388 domain.
389 The same approach of modelling was then conducted for the turbulent regime (Re > 10^5).
390 Considering this regime, foam volume is a decreasing function of the Re number, due to foam
391 collapse. From Table 1, the last 18 assays were used here to fit the Eq. 11 to the data and
392 identify the proper constants in such turbulent domain. Fig. 4b points out the correlation
393 between experimental data and predicted values through the use of the monomial equation:

394 $$\frac{H_F}{H_L} = 10^{6.25}\mathrm{Re}^{-1.32}{\Theta_m}^{0.28}\left(\frac{C_b}{H_L}\right)^{-0.06} \quad \text{Eq. 13}$$

395 In case of turbulent regime, the monomial form of the process law appears to be less accurate
396 than in case of intermediate regime (R^2 = 0.82). In the turbulent regime, the strong agitation
397 shears and breaks bubbles faster than their generation. As a result, foam collapses and final
398 volume decreases with increasing speed of agitation. As the processes interfere at a complex
399 level, it becomes arduous to describe precisely the evolution of foam volume. However, the
400 model still allows obtaining a first general understanding of the system. As for the
401 intermediate regime, the π-number related to bottom clearance is shown to have minor
402 influence on foam rate of expansion. On the other hand, the power coefficient for Reynolds
403 number is negative as observed from experimental results: an increase of Re results in a
404 decrease in foam volume. Mixing time number, Θ_m, has slightly less influence on foam
405 expansion rate in turbulent regime compared to the intermediate one, as its power coefficient
406 is a factor two lower. For this regime, and from definitions of Re and Θ_m, the expansion rate
407 is approximatively proportional to $N^{-1}{t_m}^{1/3}$, in the studied turbulent domain. This behavior
408 is far different from the intermediate regime, confirming the choice of separating the two
409 regimes for the modelling.

Both power laws obtained from dimensional analysis may be used for predicting, with a certain accuracy, the final volume of foam produced, with specific operating conditions, for SLES solutions. Master curves of foam heights for different Reynolds numbers and mixing time numbers are presented in Figure 5. To plot these curves a grid was created with different Re in the first row and different Θ_m numbers in the first column. For each couple of Re and Θ_m in the measuring range, the foam height was calculated using Eq. 12 or Eq. 13. The master curves were plotted by applying 3D map feature in Microsoft Excel 2016. The non-plotted area at the bottom right of the graph correspond to a domain not covered in this study (intermediate flow regime coupled to high mixing time number), but one could appreciate the consistency between intermediate flow regime and turbulent regime investigated. This interesting map could avoid experimental runs when a particular amount of foam is desired.

4.3. Cases of the other surfactants for intermediate regime ($10^4 < Re < 10^5$)

The experiments were also conducted in the intermediate flow regime ($10^4 < Re < 10^5$) for the two other model surfactants, Tween 20 and Brij L23. Only this regime was investigated for these two surfactants as previous results with SLES reveal that this regime was the most efficient for increasing the foaming amount. The data were compared to those of SLES in the same intermediate flow regime. As in the case of SLES, final rates of expansion showed a maximum at Reynolds numbers close to 10^5 (data not shown). Experiments also revealed that bottom clearance had minor influence on foam generation for both surfactants.

Likewise, the correlation fitting was performed for Tween 20 and Brij L23 separately, in this intermediate regime. Although fewer experimental data were available, a monomial form was found to be adequate to describe the process as well for the two surfactants, according to Eq. 9 (R^2 = 0.94 and 0.77, for Tween 20 and BrijL23 respectively). The resulting process relationships are shown in Eq. 14 and Eq. 15. These equations can be compared to Eq. 12

435 obtained for SLES in the same intermediate flow regime (10^4 < Re < 10^5). Fig. 6 showed the
436 good agreement between predicted and experimental values. As discussed before, the
437 dimensionless number describing bottom clearance effect (C_b/H_L) had no significant influence
438 on final foam expansion rate, compared to Re and Θ_m . According to the power coefficients in
439 Eq. 12, Eq. 14 and Eq.15, in the intermediate flow regime (10^4 < Re < 10^5), Reynolds number
440 has globally a higher influence on foaming ability than Θ_m and C_b/H_L whatever the surfactant.

441 Tween 20: $\frac{H_F}{H_L} = 10^{-2.0}\mathrm{Re}^{0.20}{\Theta_m}^{0.17}\left(\frac{C_b}{H_L}\right)^{0.003}$ Eq. 14

442 Brij L23: $\frac{H_F}{H_L} = 10^{-4.6}\mathrm{Re}^{0.69}{\Theta_m}^{0.28}\left(\frac{C_b}{H_L}\right)^{0.02}$ Eq. 15

443 The comparison of these three relationships to the literature is not simple because the few
444 other studies dealing with foaming in stirred tanks have been carried out in different
445 experimental domains: different vessel sizes (therefore different range of Reynolds numbers),
446 different impeller type, with gas sparging, without surfactant, etc, and most of them don't take
447 into account the effect of time (duration of agitation). However, we can noticed the
448 correlation proposed by Smith (Smith 1992) between gas hold-up and both Reynolds and
449 Froude numbers with a positive power coefficient (0.35) relative to both those dimensionless
450 numbers. If Fr number is proportional to Re^2 as in our study, the power coefficient to Re
451 number alone in Smith correlation become 1.05 which is very close to the one we obtained for
452 SLES (1.09, Eq.12).
453 To go further, and in view of direct comparison of surfactants, calculations were tried with a
454 similar set of exponent for the three different molecules. The set of exponent obtained with
455 SLES (Eq. 12) was employed as the reference and applied to experimental data of Tween 20
456 and Brij L23 in order to find a generalized process law of the form of Eq. 16:

457 $$\left(\frac{H_F}{H_L}\right) = \alpha_i\left[\mathrm{Re}^{1.09}{\Theta_m}^{0.57}\left(\frac{C_b}{H_L}\right)^{0.09}\right]^{\beta_i}$$ Eq. 16

458 with α_i and β_i constants that only depend on surfactant.

As shown in Table 2, the correlations between experimental and predicted values using Eq.16 are similar to those obtained with Eq. 12, Eq. 14 and Eq. 15, giving a sense to Eq.16. Therefore, this supports the assumption that Reynolds number and mixing time number influence in a similar way the foaming ability of surfactants solutions in that intermediate flow regime. Values of α_i and β_i obtained for each surfactant are reported in Table 2. The difference in these coefficient values can be related to own properties of each amphiphilic molecule. Namely, SLES, Tween 20 and Brij L23 have different equilibrium surface tension properties such as CMC and γ_{eq} at the CMC values. Moreover, the dynamic adsorption properties and surface viscoelasticity are known to play a major role in the formation and stabilization of foam films (Pugh 2016). Surely, the signification of these coefficients needs to be further investigated, but it was not the initial purpose of the present study.

From Eq. 16 and values in Table 2, master curves Θ_m-Re allowing to compare the three surfactants in intermediate flow regime ($10^4 < Re < 10^5$) were plotted as explained for Fig.5. These are presented in Fig. 7. SLES is globally better at foaming since it produces higher amount of foam in the studied experimental domain. Tween 20 is a poor foaming agent in these conditions whereas Brij L23 allows to produce slightly more foam.

In addition, the previous process law (Eq. 16) determined by dimensional analysis and associated master curves (Fig. 7) allow to predict the foam expansion rate for 3 model surfactants in the studied experimental domain, i.e. $3.10^4 < Re < 8.10^4$, $350 < \Theta_m < 10^4$ and $0.2 < C_b/H_L < 1$. At particular agitation speed and mixing time, dimensionless numbers involved in the foam generation process are known, and the final amount of foam can be anticipated.

5. Conclusion

In the present work, 3 model surfactants solutions were foamed in a mechanically agitated vessel according to different process parameters: agitation speed, agitation time and bottom clearance. By using the dimensional analysis approach, the foam ability of each surfactant expressed as foam expansion rate could be correlated with success to two dimensionless numbers well known in mechanical mixing processes: the Reynolds number and the mixing time number. Reynolds number was observed as mainly governing the amount of formed foam.

On the contrary, clearance bottom (C_b/H_L) of the agitator was shown to have no influence for the whole range of Reynolds covered in this study.

Thanks to the wide range of Reynolds number covered in this study, it was shown a clear difference between the intermediate flow regime ($Re < 10^5$) and the turbulent ones ($Re > 10^5$) leading to a different process law for each regime. Indeed, an increase of Reynolds number leads to an increase of foam expansion rate in intermediate flow regime but to a decrease of it in turbulent regime. In the intermediate flow regime, a general process relationships was proposed which allowed to compare the three surfactants with each other. Master curves were finally drawn showing that SLES is globally better at foaming than Tween 20 and Brij L23, the latter producing slightly more foam. In addition, those curves can be used for helping to predict final foam volumes in the studied experimental domain according to both dimensionless numbers.

This study is a first step for a better understanding and a better control of the impact of process parameters on foam ability. The next investigations should concern essentially two directions. The first one should elucidate the signification of α_i and β_i constants of the generalized law by varying the parameters relative to surfactants solutions and maybe adding new ones such as dynamic surface tension or surface viscoelasticity. As nothing guarantees that the process relationship can be written in a monomial form, or is able to adjust to the

508 “true” physical laws (which are theoretical but analytically inaccessible), second prospect of
509 this work will concern the use of other mathematical functions than monomial one in order to
510 enhance the general fit and thus provide new insights about the way the process and the
511 surfactants parameters could be involved.
512
513 **Acknowledgements**
514 This work was performed, in partnership with the SAS PIVERT, within the frame of the
515 French Institute for the Energy Transition (Institut pour la Transition Energétique (ITE)
516 P.I.V.E.R.T. (www.institut-pivert.com) selected as an Investment for the Future
517 (“Investissements d’Avenir”). This work was supported, as part of the Investments for the
518 Future, by the French Government under the reference ANR-001-01.
519
520 **References**
521
522 C. André, J. F. Demeyre, C. Gatumel, H. Berthiaux and G. Delaplace (2012). "Dimensional
523 analysis of a planetary mixer for homogenizing of free flowing powders: Mixing time and
524 power consumption." *Chemical Engineering Journal* **198-199**: 371-378 DOI:
525 http://doi.org/10.1016/j.cej.2012.05.069.

526 J. J. Bikerman (1973). Measurements of Foaminess. Foams. Springer-Verlag, Springer-Verlag
527 New York**:** 65-97.

528 M. M. Camacho, N. Martínez-Navarrete and A. Chiralt (1998). "Influence of locust bean
529 gum/λ-carrageenan mixtures on whipping and mechanical properties and stability of dairy
530 creams." *Food Research International* **31**(9): 653-658 DOI: http://doi.org/10.1016/S0963-
531 9969(99)00041-1.

532 A. Celani, S. Blackburn, M. J. H. Simmons and E. H. Stitt (2018). "Effect of mixing
533 conditions on the wet preparation of ceramic foams." *Chemical Engineering Research and*
534 *Design* **134**: 1-14 DOI: https://doi.org/10.1016/j.cherd.2018.03.044.

535 A. K. S. Chesterton, D. A. P. de Abreu, G. D. Moggridge, P. A. Sadd and D. I. Wilson (2013).
536 "Evolution of cake batter bubble structure and rheology during planetary mixing." *Food and*
537 *Bioproducts Processing* **91**(3): 192-206 DOI: http://doi.org/10.1016/j.fbp.2012.09.005.

538 V. Cristini and Y.-C. Tan (2004). "Theory and numerical simulation of droplet dynamics in
539 complex flows - A review." *Lab on a chip* **4**: 257-264 DOI: http://doi.org/10.1039/b403226h.

G. Delaplace, P. Coppenolle, J. Cheio and F. Ducept (2012). "Influence of whip speed ratios on the inclusion of air into a bakery foam produced with a planetary mixer device." *Journal of Food Engineering* **108**(4): 532-540 DOI: http://doi.org/10.1016/j.jfoodeng.2011.08.026.

G. Delaplace, Y. Gu, M. Liu, R. Jeantet, J. Xiao and X. D. Chen (2018). "Homogenization of liquids inside a new soft elastic reactor: Revealing mixing behavior through dimensional analysis." *Chemical Engineering Science* **192**: 1071-1080 DOI: http://doi.org/10.1016/j.ces.2018.08.023.

G. Delaplace, R. Guérin and J. C. Leuliet (2005). "Dimensional analysis for planetary mixer: Modified power and Reynolds numbers." *AIChE Journal* **51**(12): 3094-3100 DOI: http://doi.org/10.1002/aic.10563.

G. Delaplace, K. Loubière, F. Ducept and R. Jeantet (2015). Dimensional Analysis of Food Process, ISTE Press.

G. Delaplace, R. K. Thakur, L. Bouvier, C. André and C. Torrez (2007). "Dimensional analysis for planetary mixer: Mixing time and Reynolds numbers." *Chemical Engineering Science* **62**(5): 1442-1447 DOI: http://doi.org/10.1016/j.ces.2006.11.039.

G. Delaplace, C. Torrez, J. C. Leuliet, N. Belaubre and C. Andre (2001). "Experimental and CFD Simulation of Heat Transfer to Highly Viscous Fluids in an Agitated Vessel Equipped With a non Standard Helical Ribbon Impeller." *Chemical Engineering Research and Design* **79**(8): 927-937 DOI: https://doi.org/10.1205/02638760152721460.

P. Ding, S. Bakalis and Z. Zhang (2019). "Foamability in high viscous non-Newtonian aqueous two-phase systems composed of surfactant and polymer." *Colloids and Surfaces A: Physicochemical and Engineering Aspects* **582**: 123817 DOI: https://doi.org/10.1016/j.colsurfa.2019.123817.

W. Drenckhan and A. Saint-Jalmes (2015). "The science of foaming." *Advances in Colloid and Interface Science* **222**: 228-259 DOI: http://doi.org/10.1016/j.cis.2015.04.001.

S. M. Hall (2018). Chapter 6 - Blending and Agitation. Rules of Thumb for Chemical Engineers, 6t^{h} edition. S. M. Hall, Elsevier**:** 99-124.

W. Hanselmann and E. Windhab (1998). "Flow characteristics and modelling of foam generation in a continuous rotor/stator mixer." *Journal of Food Engineering* **38**(4): 393-405 DOI: http://doi.org/10.1016/S0260-8774(98)00129-0.

R. Hassan, K. Loubiere, J. Legrand and G. Delaplace (2012). "A consistent dimensional analysis of gas–liquid mass transfer in an aerated stirred tank containing purely viscous fluids with shear-thinning properties." *Chemical Engineering Journal* **184**: 42-56 DOI: https://doi.org/10.1016/j.cej.2011.12.066.

C. Hsu and Y. F. Maa (1996). "Microencapsulation reactor scale-up by dimensional analysis." *Journal of Microencapsulation* **13**(1): 53-66 DOI: 10.3109/02652049609006803.

B. Hu, A. W. Nienow and A. W. Pacek (2003). "The effect of sodium caseinate concentration and processing conditions on bubble sizes and their break-up and coalescence in turbulent, batch air/aqueous dispersions at atmospheric and elevated pressures." *Colloids and Surfaces B: Biointerfaces* **31**(1): 3-11 DOI: https://doi.org/10.1016/S0927-7765(03)00038-9.

L. Indrawati, Z. Wang, G. Narsimhan and J. Gonzalez (2008). "Effect of processing parameters on foam formation using a continuous system with a mechanical whipper." *Journal of Food Engineering* **88**(1): 65-74 DOI: https://doi.org/10.1016/j.jfoodeng.2008.01.015.

E. Jakubczyk and K. Niranjan (2006). "Transient development of whipped cream properties." *Journal of Food Engineering* **77**(1): 79-83 DOI: http://doi.org/10.1016/j.jfoodeng.2005.06.046.

P. Kanokkarn, T. Shiina, M. Santikunaporn and S. Chavadej (2017). "Equilibrium and dynamic surface tension in relation to diffusivity and foaming properties: Effects of surfactant type and structure." *Colloids and Surfaces A: Physicochemical and Engineering Aspects* **524**: 135-142 DOI: http://doi.org/10.1016/j.colsurfa.2017.04.043.

A. Kroezen, J. Groot Wassink and E. Bertlein (1988). Foam Generation in a Rotor-Stator Mixer.

K. Lachin, C. Turchiuli, V. Pistre, G. Cuvelier, S. Mezdour and F. Ducept (2020). "Dimensional analysis modeling of spraying operation – Impact of fluid properties and pressure nozzle geometric parameters on the pressure-flow rate relationship." *Chemical Engineering Research and Design* **163**: 36-46 DOI: https://doi.org/10.1016/j.cherd.2020.08.004.

V. Machon, A. W. Pacek and A. W. Nienow (1997). "Bubble Sizes in Electrolyte and Alcohol Solutions in a Turbulent Stirred Vessel." *Chemical Engineering Research and Design* **75**(3): 339-348 DOI: https://doi.org/10.1205/026387697523651.

P. Manjula, P. Kalaichelvi and K. Dheenathayalan (2010). "Development of mixing time correlation for a double jet mixer." *Journal of Chemical Technology & Biotechnology* **85**(1): 115-120 DOI: http://doi.org/10.1002/jctb.2274.

G. Mary, S. Mezdour, G. Delaplace, R. Lauhon, G. Cuvelier and F. Ducept (2013). "Modelling of the continuous foaming operation by dimensional analysis." *Chemical Engineering Research and Design* **91**(12): 2579-2586 DOI: http://doi.org/10.1016/j.cherd.2013.05.020.

A. H. Massey, A. S. Khare and K. Niranjan (2001). "Air Inclusion Into a Model Cake Batter Using a Pressure Whisk: Development of Gas Hold-up and Bubble Size Distribution." *Journal of Food Science* **66**: 1152-1157 DOI: http://doi.org/10.1111/j.1365-2621.2001.tb16097.x.

J. Medek and I. Fořt (1979). "Pumping effect of impellers with flat incined blades." *Collection of Czechoslovak Chemical Communications* **44**: 3078-3089 DOI: http://doi.org/10.1135/cccc19793077.

A. Mohanan, M. T. Nickerson and S. Ghosh (2020). "Utilization of pulse protein-xanthan gum complexes for foam stabilization: The effect of protein concentrate and isolate at various pH." *Food Chemistry* **316**: 126282 DOI: https://doi.org/10.1016/j.foodchem.2020.126282.

N. Müller-Fischer and E. J. Windhab (2005). "Influence of process parameters on microstructure of food foam whipped in a rotor–stator device within a wide static pressure range." *Colloids and Surfaces A: Physicochemical and Engineering Aspects* **263**(1): 353-362 DOI: https://doi.org/10.1016/j.colsurfa.2004.12.057.

N. Müller, D. Suppiger and E. Windhab (2007). "Impact of Static Pressure and Volumetric Energy Input on the Microstructure of Food Foam Whipped in a Rotor-Stator Device." *Journal of Food Engineering* **80**: 306-316 DOI: http://doi.org/10.1016/j.jfoodeng.2006.05.026.

N. Müller, P. Tobler, M. Dressler, P. Fischer and E. Windhab (2008). "Single bubble deformation and breakup in simple shear flow." *Experiments in Fluids* **45**(5): 917-926 DOI: http://doi.org/10.1007/s00348-008-0509-1.

S. Nagata, M. Yanagimoto and T. Yokoyama (1957). "A Study on the Mixing of High-viscosity Liquid." *Chemical engineering* **21**(5): 278-286 DOI: https://doi.org/10.1252/kakoronbunshu1953.21.278.

A. Patist, S. S. Bhagwat, K. W. Penfield, P. Aikens and D. O. Shah (2000). "On the measurement of critical micelle concentrations of pure and technical-grade nonionic surfactants." *Journal of Surfactants and Detergents* **3**(1): 53-58 DOI: http://dx.doi.org/10.1007/s11743-000-0113-4.

D. Pradilla, W. Vargas and O. Alvarez (2015). "The application of a multi-scale approach to the manufacture of concentrated and highly concentrated emulsions." *Chemical Engineering Research and Design* **95**: 162-172 DOI: http://doi.org/10.1016/j.cherd.2014.10.016.

R. J. Pugh (2016). Bubble and Foam Chemistry, Cambridge University Press.

M. J. Rosen, Y.-P. Zhu and S. W. Morrall (1996). "Effect of Hard River Water on the Surface Properties of Surfactants." *Journal of Chemical & Engineering Data* **41**(5): 1160-1167 DOI: http://dx.doi.org/10.1021/je960134l.

K. Samaras, M. Kostoglou, T. D. Karapantsios and P. Mavros (2014). "Effect of adding glycerol and Tween 80 on gas holdup and bubble size distribution in an aerated stirred tank." *Colloids and Surfaces A: Physicochemical and Engineering Aspects* **441**: 815-824 DOI: https://doi.org/10.1016/j.colsurfa.2013.02.031.

E. Santini, E. Jarek, F. Ravera, L. Liggieri, P. Warszynski and M. Krzan (2019). "Surface properties and foamability of saponin and saponin-chitosan systems." *Colloids and Surfaces B: Biointerfaces* **181**: 198-206 DOI: https://doi.org/10.1016/j.colsurfb.2019.05.035.

J. M. Smith (1992). Simple Performance Correlations for Agitated Vessels. Fluid Mechanics of Mixing: Modelling, Operations and Experimental Techniques. R. King. Dordrecht, Springer Netherlands**:** 55-63, DOI: https://doi.org/10.1007/1978-1094-1015-7973-1005_1007.

H. A. Stone (2003). "Dynamics of Drop Deformation and Breakup in Viscous Flows." *Annual Review of Fluid Mechanics* **26**(1): 65-102 DOI: http://doi.org/10.1146/annurev.fl.26.010194.000433.

T. Szirtes and P. Rózsa (2007). Applied Dimensional Analysis and Modeling. Burlington, Butterworth-Heinemann.

Z. Wang, F. Liu, Q. Zhang, X. Wei, D. Sun, G. Li and G. Zhang (2005). "Adsorption kinetics of Brij 35 at air/solution interface." *Indian Journal of Chemistry - Section A Inorganic, Physical, Theoretical and Analytical Chemistry* **44**(10): 2051-2054, https://www.scopus.com/inward/record.uri?eid=2-s2.0-28244477560&partnerID=40&md5=3fe4e8028a2439ee0a1d7132a95f959c.

F. White (2001). Fluid Mechanics, 7th edition, McGraw-Hill.

C. Wu, K. Nesset, J. Masliyah and Z. Xu (2012). "Generation and characterization of submicron size bubbles." *Advances in Colloid and Interface Science* **179-182**: 123-132 DOI: http://doi.org/10.1016/j.cis.2012.06.012.

J. Zhu, Z. Qian, M. Eid, F. Zhan, M. A. Ismail, J. Li and B. Li (2021). "Foaming and rheological properties of hydroxypropyl methylcellulose and welan gum composite system: The stabilizing mechanism." *Food Hydrocolloids* **112**: 106275 DOI: https://doi.org/10.1016/j.foodhyd.2020.106275.

671 M. Zlokarnik (1998). "Problems in the application of dimensional analysis and scale-up of
672 mixing operations." *Chemical Engineering Science* **53**(17): 3023-3030 DOI:
673 http://doi.org/10.1016/S0009-2509(98)00131-6.

674

Fig. 1. Illustration of a foam generation process through mechanical agitation, and physical numbers involved in the amount of created foam H_F.

Fig. 2. Evolution of foam expansion rate for SLES solution with C_b/H_L ratio, for different agitation speeds and times. Lines used as guide only.

Fig. 3. (a) Evolution of foam expansion rate with Reynolds number, for various mixing times for SLES solution. Stirring element is at the air-liquid interface ($C_b=H_L$). (b) Evolution of foam expansion rate with mixing time number (Θ_m), for different agitation speeds. Stirring element is at the air-liquid interface ($C_b=H_L$). Lines used as guide only.

Fig. 4. (a) Correlation between experimental H_F/H_L in intermediate flow regime ($Re < 10^5$) and predicted ones using Eq.12 for SLES solution. (b) Correlation between experimental H_F/H_L in turbulent regime ($Re > 10^5$) and predicted ones using Eq.13 for SLES solution 8.

Fig. 5. Master curves of H_F/H_L of SLES solution as a function of Reynolds number and mixing time number, as predicted by Eq.12 and Eq.13.

Fig. 6. Results of data modelling from Equations 14 and 15 for foam expansion rate of (a) Tween 20 and (b) BrijL23, in the intermediate flow regime; experimental domain of validity: $3.10^4 < Re < 8.10^4$, $350 < \Theta_m < 10^4$ and $0.2 < C_b/H_L < 1$.

Fig. 7. Master curves of foam rate of expansion as a function of Reynolds number and mixing time number, as predicted by Eq.16 for (a) SLES, (b) Tween 20 and (c) Brij L23, in the intermediate flow regime; experimental domain of validity: $3.10^4 < Re < 8.10^4$, $350 < \Theta_m < 10^4$ and $0.2 < C_b/H_L < 1$.

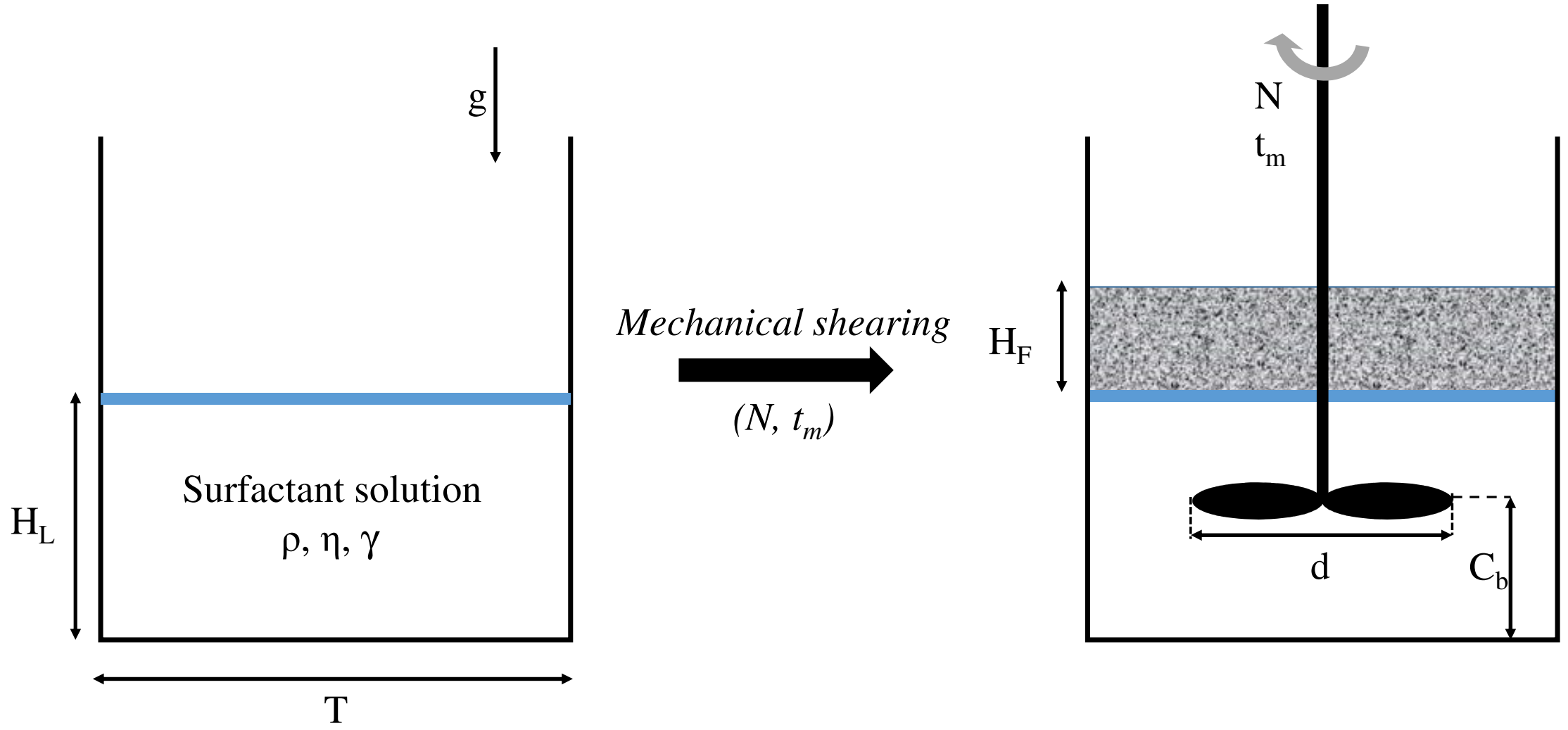
g
Surfactant solution
ρ, η, γ
H_L
T
Mechanical shearing
(N, t_m)
N
t_m
H_F
d
C_b

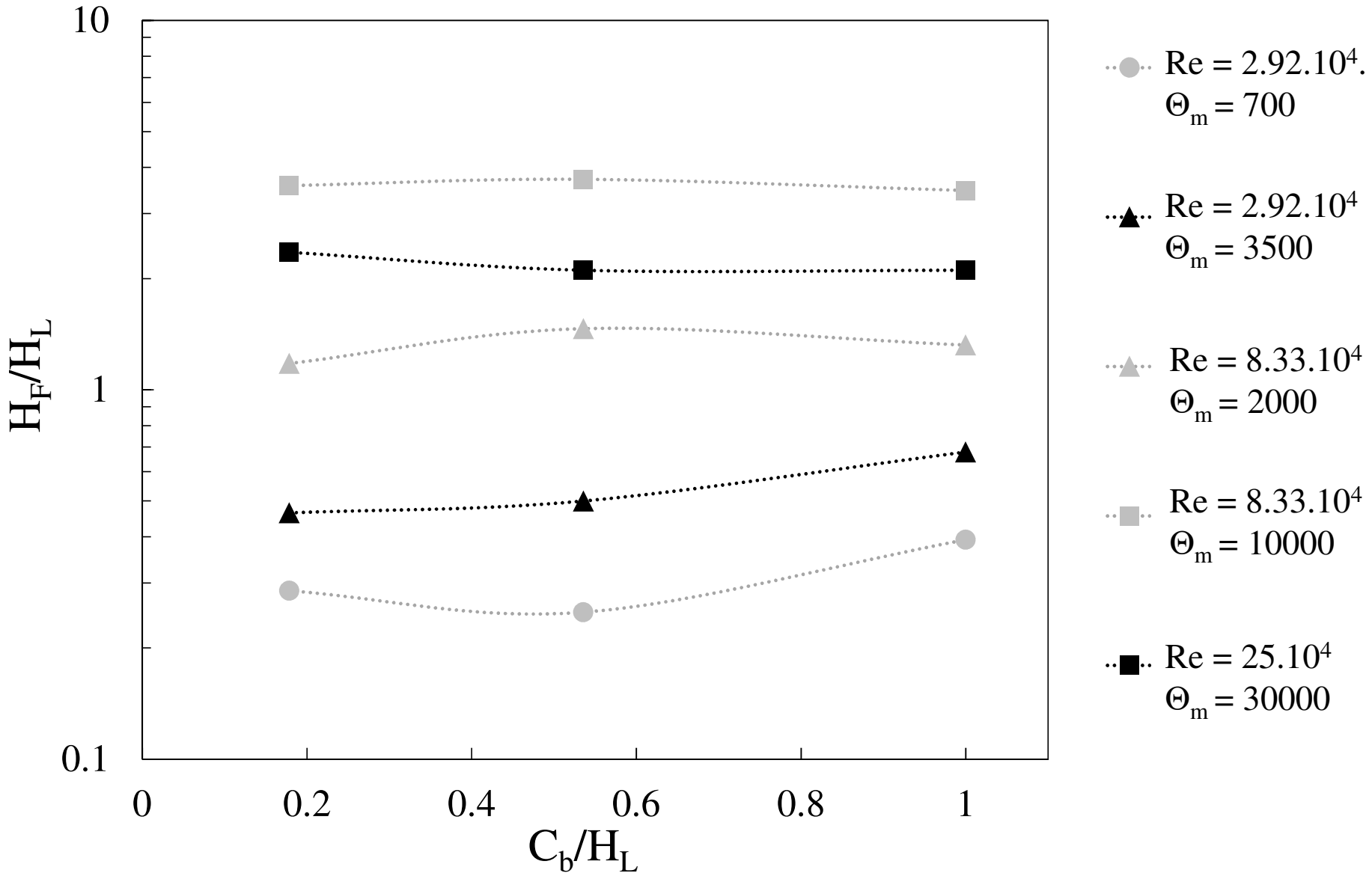
10
1
0.1
H_F/H_L
0
0.2
0.4
0.6
0.8
1
C_b/H_L
Re = 2.92.10⁴.
Θm = 700
Re = 2.92.10⁴
Θm = 3500
Re = 8.33.10⁴
Θm = 2000
Re = 8.33.10⁴
Θm = 10000
Re = 25.10⁴
Θm = 30000

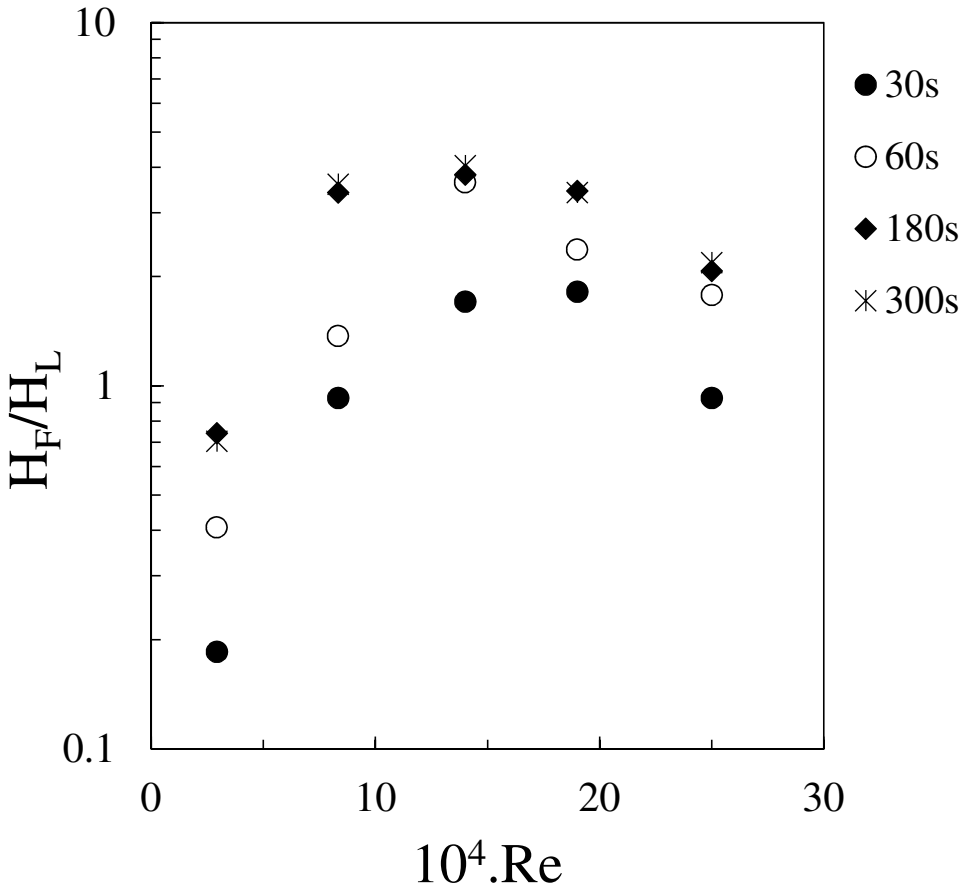
10
1
0.1
H_F/H_L
0
10
20
30
10^4.Re
30s
60s
180s
300s

(a)

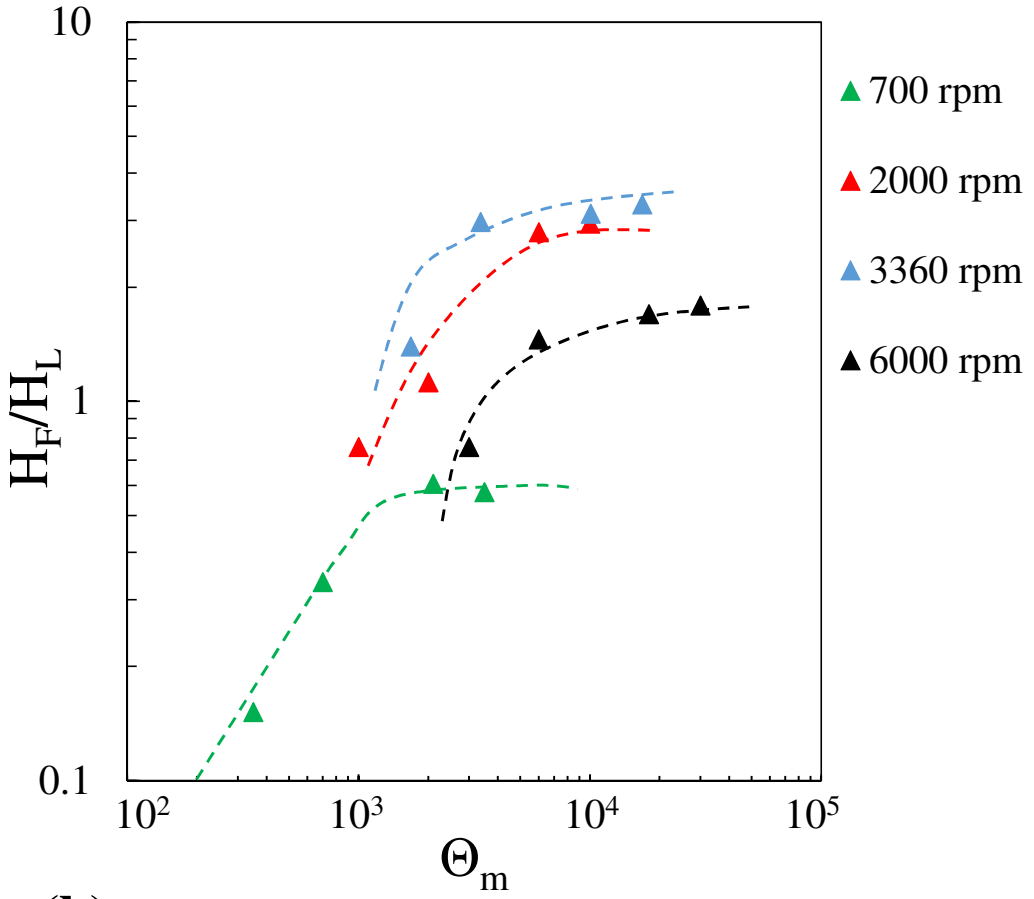
10
1
0.1
H_F/H_L
10^2
10^3
10^4
10^5
Θ_m
700 rpm
2000 rpm
3360 rpm
6000 rpm

(b)

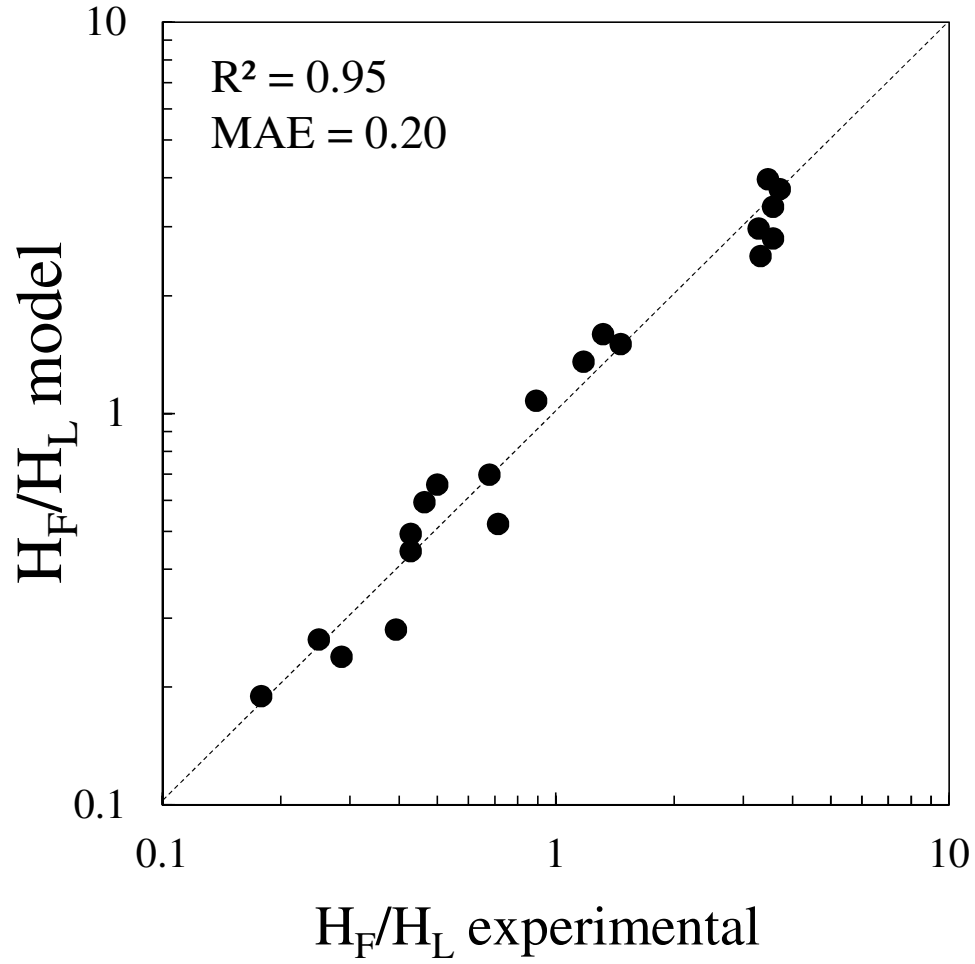
10
1
0.1
0.1
1
10
R² = 0.95
MAE = 0.20
H_F/H_L model
H_F/H_L experimental

(a)

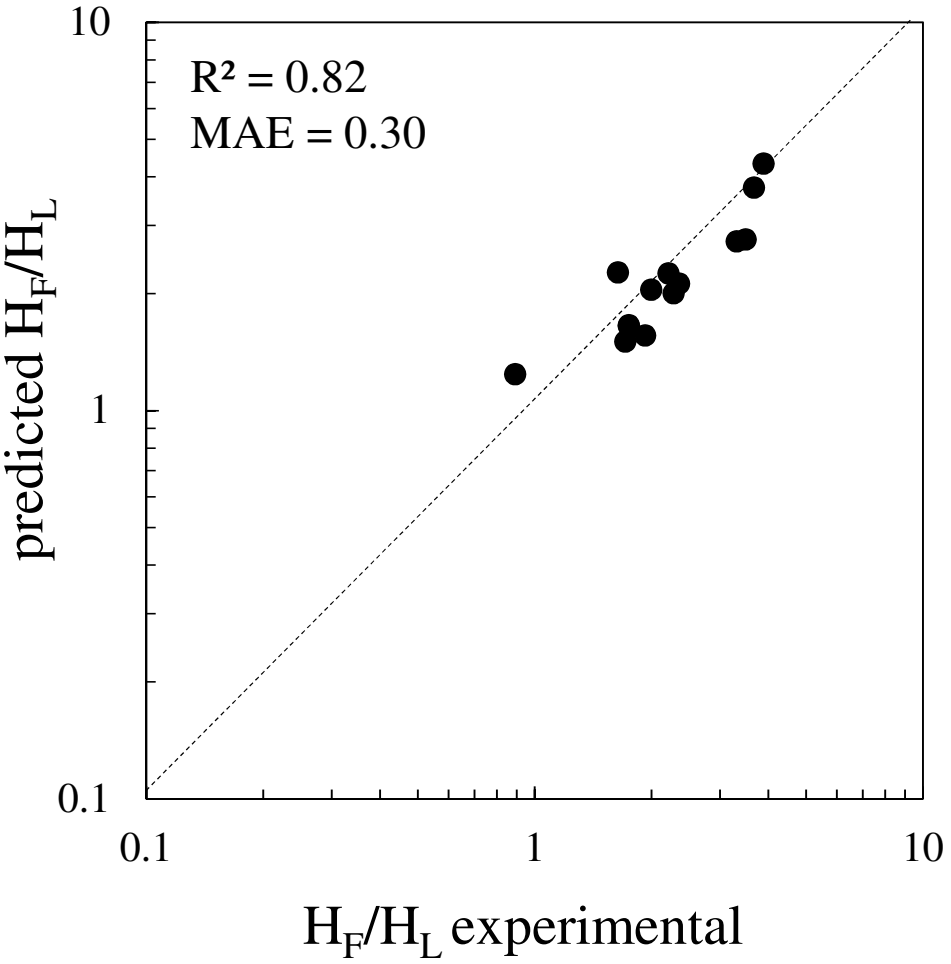
10
1
0.1
0.1
1
10
R² = 0.82
MAE = 0.30
predicted H_F/H_L
H_F/H_L experimental

(b)

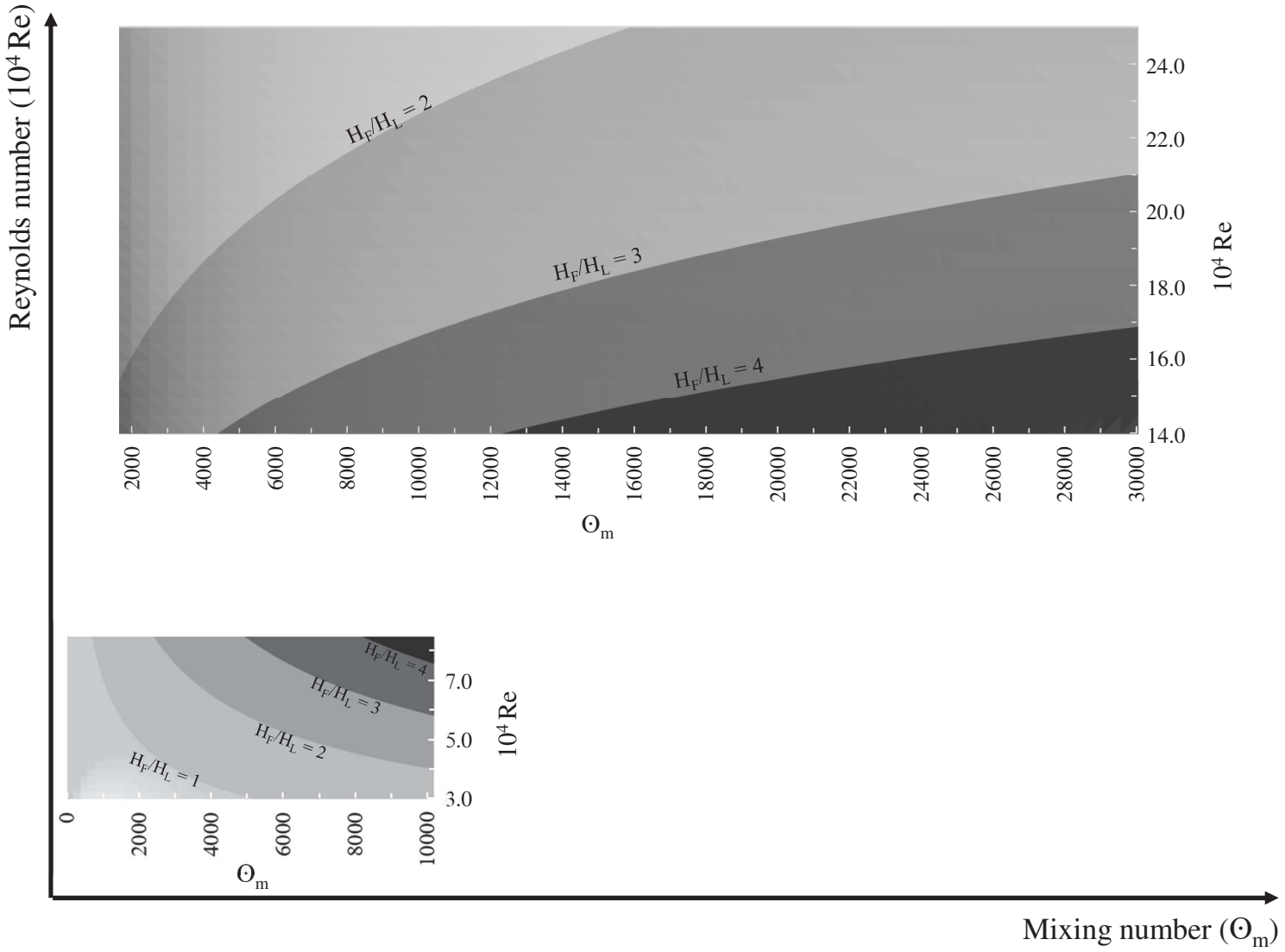
Reynolds number (10^4 Re)
$H_F/H_L = 2$
$H_F/H_L = 3$
$H_F/H_L = 4$
24.0
22.0
20.0
18.0
16.0
14.0
10^4 Re
2000
4000
6000
8000
10000
12000
14000
16000
18000
20000
22000
24000
26000
28000
30000
Θ_m
$H_F/H_L = 1$
$H_F/H_L = 2$
$H_F/H_L = 3$
$H_F/H_L = 4$
7.0
5.0
3.0
10^4 Re
0
2000
4000
6000
8000
10000
Θ_m
Mixing number (Θ_m)

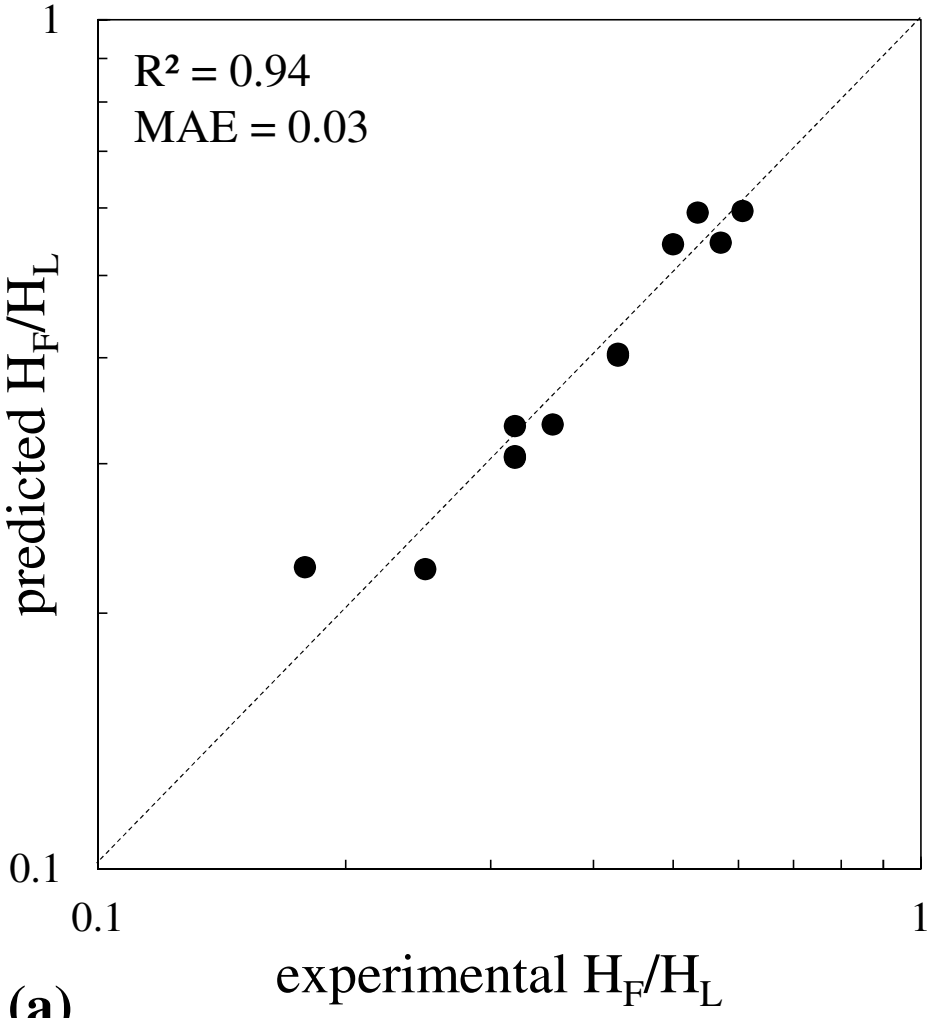
1
R² = 0.94
MAE = 0.03
predicted H_F/H_L
0.1
0.1
1
experimental H_F/H_L

(a)

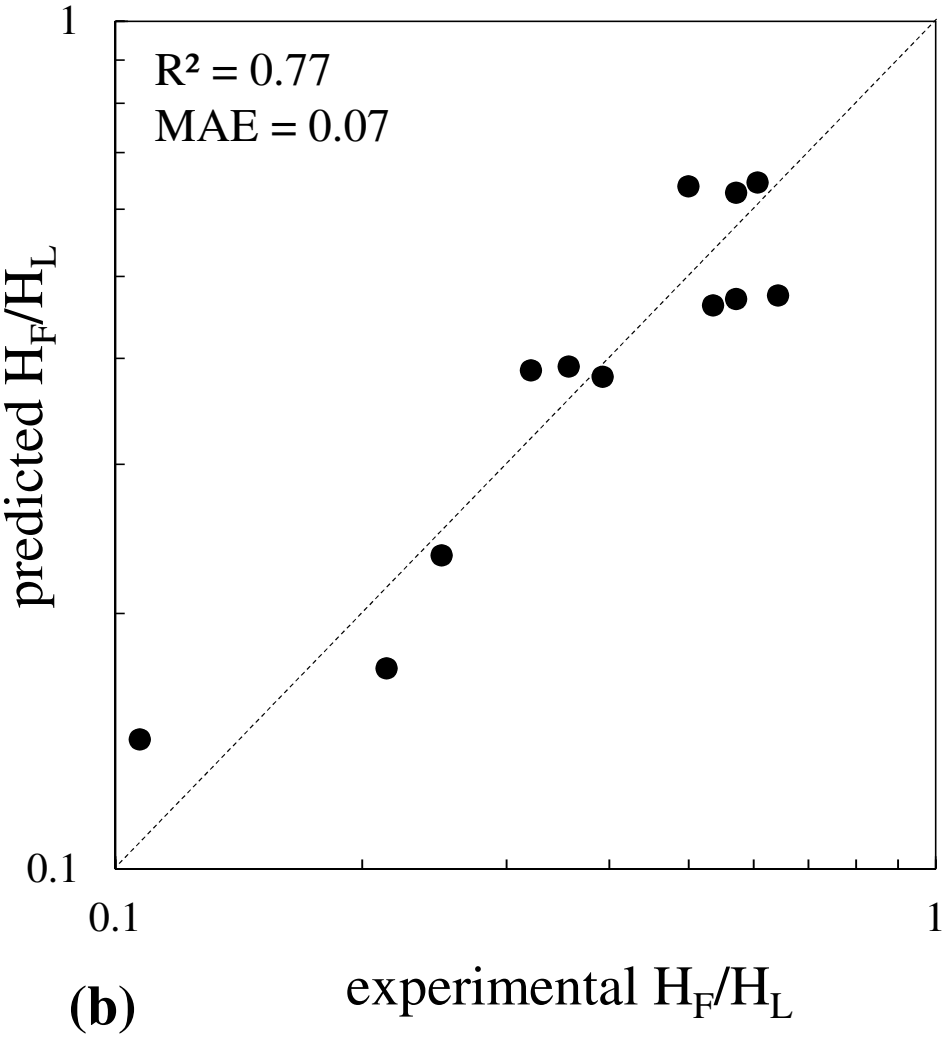
1
R² = 0.77
MAE = 0.07
predicted H_F/H_L
0.1
0.1
1
experimental H_F/H_L

(b)

(a)
$H_F/H_L = 4$
$H_F/H_L = 3$
$H_F/H_L = 2$
$H_F/H_L = 1$
7.0
5.0
3.0
10^4 Re
0
2000
4000
6000
8000
10000
Θ_m
(b)
$H_F/H_L = 0.3$
$H_F/H_L = 0.4$
7.0
5.0
3.0
10^4 Re
0
2000
4000
6000
8000
10000
Θ_m
(c)
$H_F/H_L = 0.8$
$H_F/H_L = 0.4$
7.0
5.0
3.0
10^4 Re
0
2000
4000
6000
8000
10000
Θ_m

Table 1. Foaming trials settings and experimental values of H_F, for aqueous solutions of SLES (d/H_L=1.79 and T/H_L=3.21).

Trial	Physical quantities				Dimensionless numbers				
	N (rpm)	t_m (s)	C_b (m)	H_F (m)	Re /10^4	Ca	Θ_m	C_b/H_L	H_F/H_L
1	700	30	0.028	0.005	2.92	0.02	350	1.0	0.18
2	700	60	0.005	0.008	2.92	0.02	700	0.2	0.29
3	700	60	0.015	0.007	2.92	0.02	700	0.5	0.25
4	700	60	0.028	0.011	2.92	0.02	700	1.0	0.39
5	700	180	0.005	0.012	2.92	0.02	2100	0.2	0.43
6	700	180	0.015	0.012	2.92	0.02	2100	0.5	0.43
7	700	180	0.028	0.020	2.92	0.02	2100	1.0	0.71
8	700	300	0.005	0.013	2.92	0.02	3500	0.2	0.46
9	700	300	0.015	0.014	2.92	0.02	3500	0.5	0.50
10	700	300	0.028	0.019	2.92	0.02	3500	1.0	0.68
11	2000	30	0.028	0.025	8.33	0.06	1000	1.0	0.89
12	2000	60	0.005	0.033	8.33	0.06	2000	0.2	1.18
13	2000	60	0.015	0.041	8.33	0.06	2000	0.5	1.46
14	2000	60	0.028	0.037	8.33	0.06	2000	1.0	1.32
15	2000	180	0.005	0.093	8.33	0.06	6000	0.2	3.32
16	2000	180	0.015	0.100	8.33	0.06	6000	0.5	3.57
17	2000	180	0.028	0.092	8.33	0.06	6000	1.0	3.29
18	2000	300	0.005	0.100	8.33	0.06	10000	0.2	3.57
19	2000	300	0.015	0.104	8.33	0.06	10000	0.5	3.71
20	2000	300	0.028	0.097	8.33	0.06	10000	1.0	3.46
21	3360	30	0.028	0.046	14.0	0.10	1680	1.0	1.64
22	3360	60	0.028	0.098	14.0	0.10	3360	1.0	3.50
23	3360	180	0.028	0.103	14.0	0.10	10080	1.0	3.68
24	3360	300	0.028	0.109	14.0	0.10	16800	1.0	3.89
25	4560	30	0.028	0.049	19.0	0.13	2280	1.0	1.75
26	4560	60	0.028	0.064	19.0	0.13	4560	1.0	2.29
27	4560	180	0.028	0.093	19.0	0.13	13680	1.0	3.32
28	4560	300	0.028	0.092	19.0	0.13	22800	1.0	3.29
29	6000	30	0.028	0.025	25.0	0.17	3000	1.0	0.89
30	6000	60	0.028	0.048	25.0	0.17	6000	1.0	1.71
31	6000	60	0.015	0.054	25.0	0.17	6000	0.5	1.93
32	6000	60	0.005	0.049	25.0	0.17	6000	0.2	1.75
33	6000	180	0.028	0.056	25.0	0.17	18000	1.0	2.00
34	6000	180	0.015	0.066	25.0	0.17	18000	0.5	2.36
35	6000	180	0.005	0.062	25.0	0.17	18000	0.2	2.21
36	6000	300	0.028	0.059	25.0	0.17	30000	1.0	2.11
37	6000	300	0.015	0.059	25.0	0.17	30000	0.5	2.11
38	6000	300	0.005	0.066	25.0	0.17	30000	0.2	2.36

Table 2. Constants from equation 11, R^2 and MAE for each surfactant

Surfactant	α_i	β_i	R^2 *(MAE)*
SLES	10^{-7}	1.0	0.95 *(0.20)*
Tween 20	$8.60 .10^{-3}$	0.23	0.95 *(0.02)*
Brij L23	$3.78 .10^{-5}$	0.57	0.71 *(0.07)*

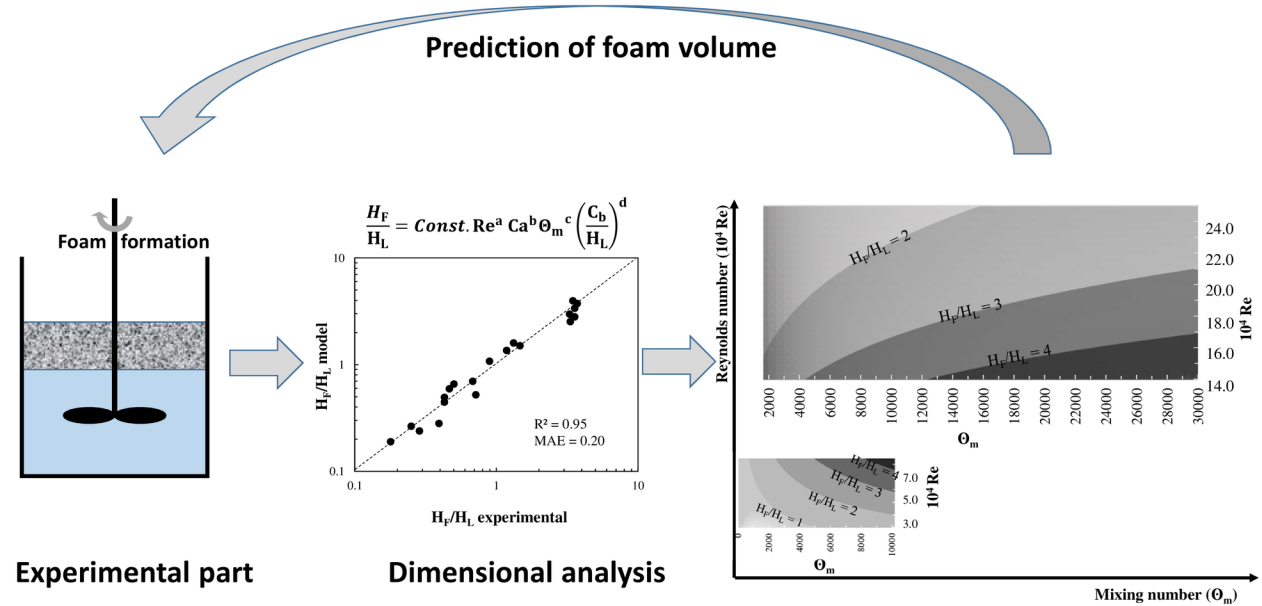
Prediction of foam volume
Foam formation
$\frac{H_F}{H_L} = Const.\,Re^a\,Ca^b\Theta_m{}^c\left(\frac{C_b}{H_L}\right)^d$
H_F/H_L model
H_F/H_L experimental
$R^2 = 0.95$
MAE = 0.20
Reynolds number (10^4 Re)
$H_F/H_L = 2$
$H_F/H_L = 3$
$H_F/H_L = 4$
$H_F/H_L = 1$
Θ_m
10^4 Re
Mixing number (Θ_m)
Experimental part
Dimensional analysis